HHS Public Access

Author manuscript

Mol Cancer Res. Author manuscript; available in PMC 2023 August 01.

Published in final edited form as:

Mol Cancer Res. 2023 February 01; 21(2): 140–154. doi:10.1158/1541-7786.MCR-22-0418.

DOT1L Regulates Ovarian Cancer Stem Cells by Activating β-catenin Signaling

Yaqi Zhang[1,2], **Yinu Wang**[1], **Andres Valdivia**[1], **Hao Huang**[1], **Daniela Matei**[1,3,4]

[1]Department of Obstetrics and Gynecology, Feinberg School of Medicine, Northwestern University, Chicago, IL 60611, USA

[2]Driskill Graduate Training Program in Life Sciences, Feinberg School of Medicine, Northwestern University, Chicago, IL 60611, USA

[3]Robert H. Lurie Comprehensive Cancer Center, Feinberg School of Medicine, Northwestern University, Chicago, IL 60611, USA

[4]Jesse Brown VA Medical Center, Chicago, IL, 60612, USA

Abstract

Cancer stem cells (CSC) represent a population of cancer cells responsible for tumor initiation, chemoresistance and metastasis. Here we identified the H3K79 methyltransferase disruptor of telomeric silencing-1-like (DOT1L) as a critical regulator of self-renewal and tumor initiation in ovarian CSCs. DOT1L was upregulated in ovarian CSCs vs. non-CSCs. shRNA-mediated DOT1L knockdown decreased the aldehyde dehydrogenase (ALDH) + cell population, impaired the tumor initiation capacity of ovarian CSCs, and blocked the expression of stemness-associated genes. Inhibition of DOT1L's methyltransferase activity by the small molecule inhibitor (DOT1Li) EPZ-5676 also effectively targeted ovarian CSCs. Integrated RNA-sequencing analyses of ovarian cancer (OC) cells in which DOT1L was knocked down vs. control cells and of ovarian CSCs vs. non-CSCs, identified Wnt signaling as a shared pathway deregulated in both CSCs and in DOT1L-deficient OC cells. β-catenin, a key transcription factor regulated by Wnt, was downregulated in OC cells in which DOT1L was knocked down and upregulated in DOT1L overexpressing OC cells. Chromatin immunoprecipitation (ChIP) revealed enrichment of the H3K79Me3 mark at the β-catenin promoter, suggesting that its transcription is regulated by DOT1L. Our results suggest that DOT1L is critical for the self-renewal and tumor initiation capacity (TIC) of ovarian CSCs by regulating β-catenin signaling. Targeting DOT1L in OC could be a new strategy to eliminate CSCs.

Introduction

Ovarian cancer (OC) is the fifth most common cancer in women and has the highest death rate among gynecological malignancies. High-grade serous ovarian cancer (HGSOC), the most common histological subtype, accounts for 70%-80% of ovarian cancer-related deaths

Corresponding Author: Daniela Matei, MD, Professor, Department of Obstetrics and Gynecology, Northwestern University Feinberg School of Medicine, 303 E Superior Street, Lurie 4-107, Tel: 312-472-4065, daniela.matei@northwestern.edu.

The authors declare no potential conflicts of interest.

(1). Although OC is initially sensitive to platinum-based chemotherapy, approximately 75% of patients experience relapse and most develop resistance to chemotherapy (2). Understanding the mechanisms regulating relapse and chemoresistance has been a priority in the field. Ovarian cancer stem cells (CSCs) are a small proportion of cells within tumors that can adapt to changes in the tumor microenvironment and survive the toxic effects of chemotherapy (3). Owing to these characteristics, CSCs have been implicated in tumor recurrence after standard therapy. Ovarian CSCs are detectable in primary ovarian tumors, in ascites, and in cell lines, and are characterized by the ability to grow as nonadherent spheroids, to self-renew, and to initiate tumors *in vivo* (4, 5). Several markers have been proposed and used to identify ovarian CSCs, including aldehyde dehydrogenase (ALDH), CD133, CD117, CD24 and CD44 (6, 7). Among them, ALDH activity is one of the most robustly validated and used markers (8, 9). It was reported that ALDH+ cells are more resistant to cisplatin and paclitaxel (10) and that chemo-resistant OC cell lines are enriched in ALDH+ OC cells (11). Additionally, ALDH1A1 expression was associated with worse clinical outcomes (12).

Epigenetic alterations and oncogenic reprogramming are important for maintaining cellular plasticity and self-renewal, hallmark traits of CSCs (13). Cancer cells harboring similar genetic features, but distinct epigenetic marks display diverse transcriptional profiles and phenotypes accounting for intra-tumoral heterogeneity. Epigenetic dysregulation, including alterations on histone modifications and DNA methylation, plays an important role in maintaining the stemness state (13). The epigenetic machinery regulates and maintains key signaling pathways, such as Wnt/β-catenin, Notch and Hedgehog, which are associated with self-renewal and stemness properties (14). Additionally, epigenetic mechanisms have been linked to the drug resistance phenotype of CSCs (15). Several recent studies examined the effects of inhibitors of epigenetic regulators in ovarian CSCs. The DNA methyltransferase (DNMT) inhibitor guadecitabine, the bromodomain and extraterminal (BET) inhibitor JQ1, and the Enhancer of Zeste 2 Polycomb Repressive Complex 2 Subunit (EZH2) inhibitor GSK126 were shown to effectively disrupt the ALDH+ cell population (16, 17). These results support that targeting epigenetic regulators could be pursued as a therapeutic strategy to eliminate CSCs.

The disruptor of telomeric silencing-1-like (DOT1L) is a histone methyltransferase that catalyzes the methylation of histone H3 on lysine-79 (H3K79), an active transcription mark (18). DOT1L is also involved in regulating RNA polymerase II-mediated transcriptional elongation, DNA damage checkpoint response, and cellular differentiation (19). Previous studies reported that DOT1L is recruited by fusion chimeras of the mixed lineage leukemia (MLL) gene, such as MLL-AF10 and MLL-AF9, which are drivers of leukemogenesis (20). Pinometostat (EPZ-5676), a small molecule DOT1L inhibitor, was shown to have inhibitory effects in preclinical models of MLL driven leukemia and is being tested in clinical trials (21). In solid tumors, DOT1L overexpression was associated with poor survival, drug resistance, and metastasis (22). DOT1L was found to be a cofactor of the estrogen receptor (ERα) and to play a role in the development of resistance to endocrine therapy in breast cancer (23). Additionally, DOT1L was shown to promote epithelial-mesenchymal transition (EMT) by cooperating with c-Myc and p300 in breast cancer cells (24) and increased

DOT1L expression was associated with poor clinical outcomes and platinum resistance in OC (25, 26).

Here we identify DOT1L as an important regulator of ovarian CSCs. We show that the expression of DOT1L was upregulated in CSCs and associated with stemness properties. Genetic depletion of DOT1L by shRNA or its pharmacological inhibition effectively reduced the ovarian CSCs population, spheroid formation and *in vivo* tumor initiation. RNA-sequencing followed by validation with ChIP-sequencing showed that DOT1L regulates the β-catenin pathway, promoting *ALDH1A1* expression. Together, our results suggest that DOT1L is critical for the survival of ovarian CSCs and could be tested as a novel therapeutic target.

Materials and Methods

Cell lines, patient-derived xenograft models, and compounds

OVCAR3 and OV90 cells were purchased from ATCC. OVCAR5 cells were obtained from Dr. Marcus Peter at Northwestern University. COV362, OVCAR4, and OVCAR8 cells were provided by Dr. Kenneth Nephew at Indiana University. Immortalized human fallopian tube luminal epithelial cells (FT190) were from Dr. R. Drapkin at University of Pennsylvania. HeyA8 cells were provided by Dr. Robert Bigsby at Indiana University. Cells were maintained at 37 °C in an environment of 5% CO2 and 100% humidity. The media used for culturing the cell lines are shown in Supplementary Table S1. Cells lines used in all experiments were at low-passages and were confirmed to be pathogen and mycoplasma-free by Charles River Animal Diagnostic Services. Cell lines were authenticated by IDEXX BioAnalytics with short tandem repeat (STR) profiling. A patient-derived xenograft (PDX) model was generated by the Developmental Therapeutics Core of the Lurie Cancer Center at Northwestern University using HGSOC tissue as previously described (11, 27). NSG mice subcutaneously implanted with second-generation PDX tumors were treated intraperitoneally with carboplatin (once/week, 15mg/kg) (Sigma-Aldrich) or PBS (control) for 6 weeks once measurable tumors of 100mm^3 were detected. Tumor volumes were monitored weekly by calipers. Tumors were harvested after 1 week after last treatment. The DOT1L inhibitor (DOT1Li) EPZ-5676 (pinometostat) was obtained from SelleckChem. Cells were treated with indicated dosages daily for 5 days and were collected on day 6 for experiments.

Human Specimens

HGSOC tumors or associated malignant ascites (n = 5) from consenting donors were collected under a Northwestern University IRB approved protocol (STU#00202468). To obtain single-cell suspensions, tumors were minced into small pieces and then digested at 37°C for 3h with 300IU/ml collagenase I (Sigma-Aldrich) and (300IU/ml) hyaluronidase (Sigma-Aldrich), as previously described (28). Cell suspensions were treated with red blood cell lysis buffer (Biolegend) and DNase I (Sigma-Aldrich) and filtered through a 40μm cell strainer (Fisher Scientific) to obtain single-cell suspension.

In vivo xenograft experiments and ELDA (extreme limiting dilution analysis)

For tumor initiation experiments, serially diluted shCtrl- and shDOT1L-transduced OVCAR5 cells (500, 1,000, 2,500) were mixed with an equal volume of Matrigel (Corning) and subcutaneously injected into female athymic nude mice (6-8 weeks old, Envigo). Length, width, and depth of tumor xenografts were measured with a digital caliper twice a week. Tumor volume was calculated with the formula volume = 1/2×length×width×depth. Mice were euthanized and tumors were harvested on day 30 after cell injection. The ELDA software (http://bioinf.wehi.edu.au/software/elda/) was used to estimate CSC frequencies in the tumors (29). The animal experiments in this study were approved by the Northwestern University Institutional Animal Care and Use Committee (IACUC, protocol #IS00003060). The platinum treated ovarian xenografts were generated by injecting subcutaneously 2 X 10^6 SKOV3 or OVCAR3 cells in the flanks of female, 8 weeks old athymic nude mice (Envigo). When xenografts were detectable and > 100 mm^3, mice were treated i.p. with PBS (control) or 25 mg/kg carboplatin, once-a-week for 3 weeks. Tumors were collected 1 week after the last treatment.

Immunofluorescence

Briefly, OVCAR5 cells were seeded on glass cover slips (Fisher Scientific) inside of a 24 well dish plate until they reach 70%-85% confluency. Cells were fixed with 4% PFA in PBS, permeabilized with 0.1% triton X-100 and blocked with BSA 2%. Cells were then incubated with primary antibodies against β-catenin (1:500, Supplementary Table S2) overnight. After incubating with secondary antibodies (Supplementary Table S2), cells were mounted on a glass slide using Flouromount with DAPI (Invitrogen). Processed cells were visualized in a Nikon A1 confocal microscope system with following settings: DAPI, emission wavelength 450 nm, excitation wavelength 405nm; Alexa Fluor 488, emission wavelength 525nm, excitation wavelength: 488nm; Alexa Fluor 568, emission wavelength 595nm, excitation wavelength 561nm. Quantification of signal was performed on Fiji software (ImageJ).

RNA sequencing (RNA-seq) and pathway enrichment analysis

Total RNA was extracted with TRI reagent (Sigma-Aldrich) and processed to remove DNA contamination using a RNase-Free DNase Set (QIAGEN). RNA concentration was measured with a NanoDrop spectrophotometer (Thermo Fisher Scientific). mRNA was isolated from 1 μg of total RNA using NEBNext Poly(A) mRNA Magnetic Isolation Module (New England Biolabs). Libraries were prepared with the NEBNext Ultra II RNA Library Prep Kit according to the manufacturer's protocol. The quality of the libraries was verified using High Sensitivity DNA Assay (Agilent Technologies) and then sequenced with an Illumina HiSeq 4000 sequencer (single-end 50bp). Raw sequences were demultiplexed with bcl2fastq Software (v2.17.1.14), and after quality evaluation with the FastQC tool, sequences were aligned to the human genome build hg38 using STAR (v.2.5.2) software. Mapped reads were processed to raw counts with the HTSeq tool. The edgeR (Bioconductor) package was used to normalize the counts (based on library size) and to determine differentially expressed genes. Pathway enrichment analysis was performed by using MetaCore (https://portal.genego.com, Clarivate) with standard settings. Gene Set Enrichment Analysis (GSEA) was performed by uploading the log2 (Fold change) and

P-values of normalized counts in each group and analyzed with standard settings. Data were deposited in GEO, GSE 199472.

TCGA data analysis, Kaplan-Meier survival analysis

Correlations were calculated between *DOT1L* and *CTNNB1* gene expression levels (RNA-seq) in HGSOC specimens (n=427) from The Cancer Genome Atlas (TCGA) database (30). RSEM counts were downloaded from UCSC Xena Browser (https://xenabrowser.net/) and analyzed as described above. Kaplan-Meier survival analyses were performed using an online tool https://kmplot.com/analysis/) with a database combined gene expression data and overall survival information of ovarian patients downloaded from Gene Expression Omnibus (GEO) and TCGA (Affymetrix HG-U133A, HG-U133A 2.0, and HG-U133 Plus 2.0 microarrays) (n = 655) (31). The microarray probe "226201_at" was used in this analysis, and a total of 655 samples from GEO were analyzed, including GSE18520, GSE19829, GSE26193, GSE27651, GSE30161, GSE63885, and GSE9891. The statistical significance of survival differences between groups with high vs. low *DOT1L* levels of expression was determined using the log-rank test.

Detailed protocols for the lentiviral knockdown, flow cytometry and fluorescence-activated cell sorting (FACS), plasmid construction and establishment of overexpressing cells, TOPFlash luciferase assay, spheroid formation assay, clonogenic survival assay, quantitative real-time PCR, Western blotting, CCLE data analysis, immunohistochemistry (IHC), chromatin immunoprecipitation (ChIP) and ChIP-sequencing (ChIP-seq) are included in Supplementary Materials and Methods.

Statistical analysis

Data are presented as means ± standard deviation (SD). Statistical significance was determined by using two-tailed Student's t test (Prism 8, Graphpad Software). A P value < 0.05 indicates statistical significance. The Kaplan-Meier method with log-rank and Cox's proportional hazard regression model was used to calculate overall survival (OS).

Data availability

All high-throughput sequencing data and processed data have been deposited in the National Center for Biotechnology Information (NCBI) Gene Expression Omnibus (GEO) data repository: GSE199474. The analysis was performed by using publicly available software described in methods.

Results

DOT1L is enriched in ALDH+ ovarian CSCs

To investigate the role of DOT1L in ovarian CSCs, we measured its *mRNA* expression levels in sorted ALDH+ CSCs and ALDH− cells from human HGSOC tumors. *DOT1L* was significantly upregulated in ALDH+ cells compared with ALDH− cells ($p = 0.03$, n = 6, Fig. 1A). Similarly, upregulation of *DOT1L* was observed in ALDH+ CSCs vs. ALDH− cells sorted from OC cell lines OVCAR5 and COV362 (Fig. 1B). DOT1L protein and amounts of H3K79Me3, the product of DOT1L histone methyltransferase activity, were both increased

in ALDH+ relative to ALDH− cells sorted from OVCAR5 cells (Fig. 1C). RNA-seq analysis of ALDH+CD133+ vs ALDH−CD133− cells sorted from OVCAR5 also showed elevated *DOT1L* expression in ovarian CSCs (Fig. 1D).

To verify the expression of DOT1L in cancer vs. normal tissue and relative to the stem cell population, we measured the amounts of *DOT1L mRNA* in multiple OC cell lines and in the non-malignant fallopian tube epithelial cells (FT190) (Fig. 1E). DOT1L was upregulated in all OC cell lines compared with FT190 cells. We further analyzed the expression of *DOT1L* and total ALDH genes (including 18 ALDH isoforms) in 47 OC cell lines included in the Cancer Cell Line Encyclopedia (32). As shown in Fig. 1F, the expression levels of DOT1L were positively correlated with total levels of ALDH isoforms ($Y = 4.836*X+96617$, $p = 0.0480$, Pearson $r = 0.29$). Survival analysis using the gene expression data from 655 OC patients from GEO database indicated that patients whose tumors harbor high *DOT1L* levels had shorter overall survival (OS) compared with patients with tumors displaying low *DOT1L* expression (top 25 percentile, n = 164 vs. bottom 25 percentile, n = 164; $p = 0.0058$, Fig. 1G).

Previous studies have shown that ovarian tumors from chemotherapy-treated patients are enriched in ALDH+ cells, correlating with chemoresistance and poor clinical outcomes (6, 33). To determine whether platinum chemotherapy alters *DOT1L* expression, mice bearing OVCAR3 or SKOV3 xenografts were treated with carboplatin weekly and the expression of *DOT1L* and of the stemness marker *ALDH1A1* was measured in harvested tumors residual after carboplatin treatment and compared with xenografts from mice treated with PBS (control). Both *DOT1L* and *ALDH1A1* were upregulated in carboplatin treated relative to control tumors (Fig. 1H), reflecting an increase in DOT1L expression in conjunction with CSC enrichment induced by carboplatin. Similarly, DOT1L protein (IHC) and *mRNA* (qRT-PCR) levels were measured in ovarian PDXs residual after treatment with 6 weekly cycles of carboplatin. DOT1L protein and *mRNA* expression levels were increased in tumors residual after carboplatin compared to control tumors (Figs. 1I–J, $p = 0.0137$). In summary, high DOT1L expression is associated with stemness features, decreased PFS, and an increase in CSCs induced by platinum.

DOT1L regulates the functions of ALDH+ CSCs

To establish the functions of DOT1L in ovarian CSCs, we generated DOT1L-knockdown cells (shDOT1L) by transducing OVCAR5 and COV362 cells with two shRNAs sequences targeting *DOT1L*. Knockdown efficiency was validated by measuring *DOT1L mRNA* level by qRT-PCR (Fig. 2A) as well as DOT1L and H3K79Me3 protein levels by western blotting (Fig. 2B). The ALDH+ CSCs population was measured in shDOT1L and control (shCtrl) cells by flow cytometry with ALDEFLUOR assay. The percentages of ALDH+ cells were decreased in OVCAR5 and COV362 cell lines transduced with shRNA targeting DOT1L vs. control (Fig. 2C, D, OVCAR5 $p = 0.0202$ and $p = 0.0046$; COV362 $p = 0.0026$ and $p = 0.0078$). Consistent with these results, *in vitro* tumor sphere-forming assay indicated that shDOT1L cells formed fewer and smaller size spheres than shCtrl cells (Fig. 2E, F, OVCAR5 $p = 0.0012$ and $p < 0.0001$; COV362 $p < 0.0001$ and $p < 0.0001$). To assess the effect of DOT1L knockdown on TIC, we injected low numbers (2,500; 1,000; 500) of

shDOT1L or shCtrl OVCAR5 cells, subcutaneously into female nude mice. TIC was delayed in mice injected with shDOT1L compared with shCtrl cells at all concentrations (total of 10/12 in shCtrl vs 2/12 in shDOT1L at Day16, $p = 0.0004$, Supplementary Table S6). Extreme limiting dilution analysis (ELDA) calculations (29) showed that tumors initiated from DOT1L depleted OVCAR5 cells (shDOT1L) harbored lower stem cell frequency compared with tumors induced by shCtrl cells (Figs. 2G and Supplementary Table S7, $p = 0.0001$). Furthermore, xenografts derived from shDOT1L cells were smaller in size over time as compared to tumors derived from control cells (Supplementary Fig. S1A). The percentages of ALDH+ CSCs in cells derived from shDOT1L xenografts were significantly decreased compared to cells isolated from control xenografts (Fig. 2H, $p = 0.0138$). Likewise, spheroid formation by single cell suspensions isolated from shDOT1L xenografts was inhibited when compared with control xenografts (Fig. 2I and Supplementary Fig. S1B).

To verify the role of DOT1L in stemness, we also overexpressed DOT1L in OVCAR5 and COV362 cells (DOT1L-OE) by stably transducing cells with a DOT1L-expressing vector (Supplementary Fig. S1C, D). The ALDH+ CSCs population was measured by FACS (Supplementary Fig. S1E, $p = 0.0335$ in OVCAR5 and $p = 0.0120$ in COV362), and the sphere-forming ability (Supplementary Figs. S2F, $p < 0.0001$ in OVCAR5 and COV362) were significantly increased in DOT1L-OE cells compared with cells transduced with empty vector (EV). These data support an important role of DOT1L in maintaining OC stemness.

DOT1L regulates the expression of stemness-associated genes in ovarian CSCs

Previous research showed that ALDH+ ovarian CSCs have upregulated expression of stemness-associated transcriptional factors (*SOX2*, *OCT4*, *NANOG*) and of the stemness marker *ALDH1A1*. We examined how DOT1L expression altered the transcription of those genes. DOT1L knockdown in OVCAR5 and COV362 cells significantly reduced the expression of stemness-associated genes *SOX2*, *OCT4*, *NANOG* and *ALDH1A1* (Fig. 3A, $p < 0.05$). Conversely, expression of the stemness-associated genes was upregulated in DOT1L-OE compared with EV transduced cells (Fig. 3B, $p < 0.05$).

To identify DOT1L target(s) among the genes involved in cell stemness, we performed RNA-sequencing analysis in OVCAR5 cells transduced with shRNA targeting DOT1L vs. control. A total of 7308 genes were differentially expressed in shDOT1L vs. shCtrl cells (FDR < 0.05), of which 3547 genes were downregulated and 3761 were upregulated (Supplementary Tables S8–9). A volcano plot (Fig. 3C) shows differentially expressed genes between OVCAR5 cells transduced with shRNA targeting DOT1L vs. control, including *ALDH1A1, ALDH1A3, ALDH2*, and other genes related to stemness. We then examined the expression profiles of the 84 genes included in the "cancer stem cell module" of the Ingenuity Pathway Analysis software. A heatmap showing the top 25 downregulated genes after DOT1L knockdown is illustrated in Fig. 3D. This cluster includes previously reported stemness-associated genes in cancer such as *ALDH1A1, CD24, CD44, NOTCH1, NOTCH2* and *STAT3*. Gene Set Enrichment Analysis (GSEA) identified significant enrichment in the "*Boquest stem cell up*" module and "*Lim mammary stem cell up*" modules in shDOT1L compared with shCtrl cells. These are gene sets related to stromal stem cells and mammary stem cells, respectively (Fig. 3E, Supplementary Fig. S1G) (34, 35). We also identified

reduced enrichment of "*Hallmark of epithelial-mesenchymal transition*" (M5930) GSEA gene set in shDOT1L cells vs shCtr cells (Fig. 3F). These analyses indicate that DOT1L knockdown significantly altered the expression of stemness-associated genes in OC cells.

A DOT1L inhibitor (DOT1Li) reduced the ovarian CSC population and expression of stemness-associated genes

To verify the effects of DOT1L inhibition, we next treated ovarian cancer cells with EPZ-5676, a specific inhibitor of DOT1L methyltransferase activity. The inhibition efficacy of EPZ-5676 was assessed by measuring levels of H3K79Me2/3 by western blotting. Treatment of OVCAR5 cells with as low as 100 nM and up to 10 μM DOT1Li effectively inhibited total H3K79Me3 levels, and to a lesser degree H3K79Me2 (Fig. 4A, Supplementary Fig. S2A). OVCAR5 and COV362 cells treated with DOT1Li formed fewer spheroids under low-attachment culture conditions (Fig. 4B, C, $p < 0.05$), while the proliferation rate of cells grown as monolayers for 96 hours was not affected by DOT1L inhibition (Supplementary Fig. S2B), implying that treatment with DOT1Li reduced sphere-forming capacity rather than directly inhibiting cell growth. Consistent with the results obtained by testing cell lines, cells isolated from HGSOC human tumors formed fewer spheroids when treated with DOT1Li (Fig. 4D, $p < 0.05$), demonstrating the clinical relevance of our findings. Furthermore, treatment with DOT1Li inhibited clonogenicity in three cell lines measured by an *in vitro* clonogenic survival assay, indicating the inhibitor decreased proliferation initiated from low cell numbers (Fig. 4E, Supplementary Fig. 2C, $p < 0.05$). In addition to decreasing spheroid forming and clonogenicity abilities, DOT1Li treatment also significantly reduced ALDH+ cell population in OC cells (Figs. 4F–G, OVCAR5 $p = 0.042$ and COV362 $p = 0.001$). Expression of stemness-associated genes (*SOX2, OCT4, NANOG* and *ALDH1A1*) was also reduced by treatment with DOT1Li in OVCAR5 and COV362 cells (Fig. 4H–I, $p < 0.05$). Together, these results show that inhibition of DOT1L enzymatic function reduces stemness in OC cells, similar to the effects observed with DOT1L depletion by shRNA.

DOT1L regulates the stemness features of ovarian CSCs by upregulating β-catenin

To determine the mechanism by which DOT1L regulates cancer stemness, we performed pathway enrichment analysis by using Metacore on the differential expressed genes (DEGs) in shDOT1L vs shCtrl OVCAR5 cells. The Wnt canonical pathway was identified as the top altered pathway in this analysis, with 48 genes out of the 77 genes included in the pathway being differentially expressed between the groups (Fig. 5A). To determine if the Wnt pathway is associated with the CSCs subpopulation in OVCAR5 cells, we performed pathway enrichment analysis on the shared DEGs between two RNA-sequencing datasets: the comparison between OVCAR5 cells transduced with shRNA targeting *DOT1L* vs cells transduced with control shRNA (GSE199472), and ALDH+ CSCs vs ALDH− non-CSCs (GSE148003, Supplementary Fig. S3A). Pathway analysis of the common (overlapping) DEGs between these two RNA-seq based datasets identified Wnt as the top altered pathway. To further verify the relationship between DOT1L and canonical Wnt signaling pathway, we analyzed the genes that are dependent on DOT1L expression among 33 OC cell lines profiled by the DepMap database (36). According to the dependency rank relative to DOT1L, 18 genes from the KEGG Wnt canonical signaling pathway (hsa04310) were

highly dependent on DOT1L in the 33 OC cell lines profiled, suggesting a strong correlation between DOT1L and Wnt signaling (Fig. 5B).

We then examined the expression of genes in the KEGG Wnt canonical signaling pathway (hsa04310) in the dataset comparing OVCAR5 shDOT1L vs shCtrl cells. A heatmap (Fig. 5C) shows 67 DEGs, with the majority been downregulated in cells depleted of DOT1L. Analysis by GSEA also showed decreased enrichment of the "WNT UP. V1" geneset in shDOTL1 compared with shCtrl OVCAR5 cells (Supplementary Fig. S3B). Among these genes, β-catenin (*CTNNB1*), the key transcriptional factor in the Wnt pathway, which had been previously identified as regulator of *ALDH1A1* in OC cells (8), was downregulated in shDOT1L cells compared with control cells. Furthermore, the expression levels of *DOT1L* and *CTNNB1* genes were significantly correlated in the HGSOC specimens from TCGA dataset (Fig. 5D, Pearson r = 0.7046, $p < 0.0001$). Additionally, RNA-sequencing compared ALDH+ CSCs treated with DOTLi (100nM for 5 days) vs. control. Among the DEGs between groups, the module *"FEVR CTNB1 TARGET DN*" containing target genes of β-Catenin was significantly enriched, further supporting that not only genetic depletion, but also enzymatic inhibition directly affects this stemness-associated pathway (Supplementary Fig. S3C). *CTNNB1 mRNA* levels measured by q-RT-PCR were decreased in shDOT1L vs shCtrl cells in OVCAR5 and COV362 cell lines (Fig. 5E). Reversely, *CTNNB1* expression levels were increased in OVCAR5 and COV362 cells overexpressing DOT1L compared to control cells (Supplementary Fig. S3D). The protein levels of β-catenin and its downstream targets, ALDH1A1 and Cyclin D1, were also decreased in shDOT1L vs. shCtrl cells, and increased in cells overexpressing DOT1L vs. control cells (Fig. 5F). The expression levels of *CTNNB1, CCND1* and *ALDH1A1* were also consistent with the changes in corresponding protein (Fig. 5G). Collectively these results support that DOT1L regulates stemness by altering β-catenin expression and signaling.

DOT1L regulates β-catenin expression by affecting H3K79 methylation at its promoter region

To determine whether DOT1L exerts epigenetic regulation of β-catenin, we mapped the H3K79Me3 histone marks deposited by DOT1L by using ChIP-sequencing with an antibody against H3K79Me3 in OVCAR5 cells. H3K79Me3 deposition was enriched in the proximal promoter region of the *CTNNB1* gene (Fig. 6A). To confirm this observation, we performed ChIP quantitative PCR in cells depleted of DOT1L. A significant reduction in H3K79Me3 deposition in the *CTNNB1* promoter region was observed between shDOT1l and control cells (Fig. 6B, $p = 0.0098$), supporting that DOT1L epigenetically regulates the transcription of β-catenin by altering the deposition of the active H3K79Me3 mark at its promoter.

Canonical Wnt signaling pathway involves translocation of β-catenin into the nucleus causing its interaction with the transcriptional elements TCF/LEF to induce expression of target genes. To assess whether DOT1L affects the functions of b-catenin, we measured its activity by using the TOPFlash reporter assay (34)) and its nuclear translocation in shDOT1L compared to control cells. As hypothesized, β-catenin activity measured by the TOPFlash assay was reduced in DOT1L knockdown cells (Fig. 6C, $p = 0.0120$) and in cells treated with DOT1Li compared to control cells (Fig. 6C, $p = 0.0051$). Immunofluorescence

(IF) staining demonstrated decreased nuclear translocation of β-catenin in shDOT1L vs. shCtrl cells, likely due to less amounts of total β-catenin in the knockdown cells (Supplementary Fig. S3E). OVCAR5 cells were then treated with the ligand Wnt-3a which promotes nuclear translocation of β-catenin. Nuclear translocation of β-catenin in response to Wnt-3a was detected in shCtrl cells (Fig. 6D). Although β-catenin also partly translocated to the nucleus in shDOT1L cells treated with Wnt-3a, colocalization levels were reduced compared to the control group, suggesting that the nuclear β-catenin was decreased by DOT1L depletion (Fig. 6D and 6F). Quantification of fluorescence intensity in shDOT1L vs. shCtrl cells indicated the significant reduction of total cellular β-catenin levels (Fig. 6E) as well as of nuclear levels (Fig. 6F). Collectively, the results support that DOT1L regulates the expression levels of β-catenin, impacting a key stemness-related pathway in OC.

To validate the significance of β-catenin downstream of DOT1L, we overexpressed β-catenin in sh-DOT1L stably transduced OVCAR5 cells. Expression levels of β-catenin were quantified by q-RT-PCR (Fig. 7A). Overexpression of β-catenin rescued the expression of *ALDH1A1* (Fig. 7B) and percentage of ALDH+ cells (Fig. 7C) to similar levels as in shDOT1L stably transduced OVCAR5 cells to baseline levels in shCtrl transduced cells. Likewise, overexpression of β-catenin restored spheroid formation capacity in cells depleted of DOT1L (Figs. 7D and E). The data support the role of β-catenin as a key factor regulating stemness downstream of DOT1L.

Discussion

Epigenetic regulators, especially histone modifiers, are associated with tumor initiation, disease progression, and response to chemotherapy. In this study, we identified the H3K79 methyltransferase DOT1L as a critical regulator of ovarian CSCs. First, we found the enrichment of DOT1L in ovarian CSCs from HGSOC tumors and ovarian cancer cell lines. Second, we showed that DOT1L targeting either by shRNA depletion or by enzymatic inhibition alters the CSCs population. Third, we identified the Wnt/β-catenin signaling as the major downstream target of DOT1L promoting stemness.

Our results unveil a previously unreported function of DOT1L in regulating ovarian CSCs. Previous studies reported that DOT1L is associated with OC cell proliferation through alterations in nucleotide and amino acid metabolic pathways (26) and with platinum-resistance through activation of the transcription factor CCAAT/Enhancer Binding Protein (C/EBP) complex (37). Here we report higher expression levels of DOT1L in ovarian CSCs vs non-CSCs and found that the methyltransferase was upregulated in post-chemotherapy ovarian tumors, which are enriched in ALDH+ CSCs. Additionally, DOT1L expression was strongly associated with the ALDH+ CSC populations in OC cell lines. Knockdown by shRNA or inhibition by the small molecule inhibitor EPZ-5676 effectively reduced the ALDH+ population, inhibited the expression of stemness-associated genes and blocked TIC *in vivo*. The methyltransferase was linked to cancer stemness in other contexts. For example, DOT1L was shown to induce the expression of stem cell transcription factors *NANOG*, *SOX2* and *OCT4* in colon cancer cells treated with IL22 (38) and to be highly expressed in CSCs derived from glioblastoma (39). Another recent study showed that inhibition of DOT1L by EPZ-5676 decreased stemness characteristics in triple negative breast cancer

(40). However, these studies and our findings contrast with a previous report which showed that CRISPR-mediated DOT1L knockout promoted cell invasion and increased the numbers of CSC and ALDH expression (41). The conflicting data could be related to adaptive mechanisms triggered by the complete knock out of the methyltransferase or to the more limited cell models used in that report. In all, the newly described functions of the methyltransferase in ovarian CSCs highlight the potential importance of developing an inhibitory strategy for DOT1L in OC.

From the transcriptomic analyses performed, we identified the Wnt/β-catenin signaling as the major target of DOT1L in CSCs. By using ChIP, TOPflash reporter assay and immunofluorescence staining, we demonstrated activation of β-catenin by DOT1L. Analysis of publicly available genomic data from the TCGA and DepMap database confirmed the association between DOT1L and β-catenin expression levels. β-catenin had been reported to be a critical regulator of cancer stemness in platinum-resistant HGSOC (42). Our group had also reported that β-catenin directly binds to the promoter of ALDH1A1 regulating its expression of *ALDH1A1* (8). Higher β-catenin activity had been reported in HGSOC, although mutations in *CTNNB1* or of components of the β-catenin destruction complex are uncommon (43). Previous studies have proposed alternative mechanisms leading to Wnt/β-catenin activation in OC, such as upregulation of the ligands Wnt5A or Wnt7A (44) or abnormal dissociation of β-catenin and E-cadherin, mediated by the tissue transglutaminase (45). Epigenetic mechanisms have also been reported to activate β-catenin. Dickkopf related protein 2 (DKK2), an antagonist of Wnt signaling, was found to be downregulated in OC through promoter methylation (46). Here, we unveil a novel epigenetic mechanism that mediates upregulation of β-catenin in OC: DOT1L is enriched in ovarian CSCs and promotes the enrichment of the active histone mark H3K79Me3 at the *CTNNB1* promoter, activating its transcription.

Our results examining the effects of DOT1Li EPZ-5676 shed light on the potential of targeting this methyltransferase for clinical applications. EPZ-5676 was previously tested in MLL-rearranged acute leukemia, showing an acceptable safety and tolerability profile, although treatment efficacy was modest (21). One major limitation of the existing inhibitor is its pharmacokinetic profile, with a short half-life, requiring continuous intravenous delivery to achieve sustained exposure of cancer cells to the drug (21). This limitation delayed the development of DOT1L inhibitors for solid tumors. Another shortcoming of small molecule epigenetic inhibitors is their indiscriminate actions across the genome, contributing to potential toxicities and non-specific effects (47). Although epigenetic interventions have garnered an interest in recent years for solid tumors, including OC, with ongoing clinical testing of inhibitors for DNA methyltransferases (decitabine and guadecitabine) (48, 49) or for histone deacetylases (HDAC, belinostat) (50), results have remained inconclusive and these agents have not yet succeeded entering the clinical space. Here we show the inhibitory effects of the DOT1L inhibitor against treatment resistant CSCs. Similar efficacy was shown in a previous study targeting platinum-resistant ovarian tumors (26). In all, our results suggest that DOT1L is a critical epigenetic modifier required for maintaining the stemness properties of ovarian CSCs through regulation of β-catenin. The data support further preclinical testing and chemical optimization of DOT1L inhibitory strategies to enable successful applications in the clinic.

Supplementary Material

Refer to Web version on PubMed Central for supplementary material.

Acknowledgements

This research was supported by funding from the US Department of Veterans Affairs (BX000792-09A2), NCI U54 CA268084-02 and the Diana Princess of Wales endowed Professorship from the Lurie Cancer Center to DM. Tumor specimens were procured through the Tissue Pathology Core and sequencing was performed in the NUSeq Core supported by NCI CCSG P30 CA060553 awarded to the Robert H Lurie Comprehensive Cancer Center. Flow cytometry analyses were performed in the Northwestern University - Flow Cytometry Core Facility supported by Cancer Center Support Grant NCI CA060553. Imaging of TMA was performed in the Center for Advanced Microscopy/Nikon Imaging Center (CAM) at Northwestern University supported by NCI CA060553. This research was supported in part through the computational resources and staff contributions provided for the Quest high performance computing facility at Northwestern University which is jointly supported by the Office of the Provost, the Office for Research, and Northwestern University Information Technology.

References

1. Siegel RL, Miller KD, Jemal A. Cancer statistics, 2020. CA Cancer J Clin. 2020;70(1):7–30. [PubMed: 31912902]
2. du Bois A, Reuss A, Pujade-Lauraine E, Harter P, Ray-Coquard I, Pfisterer J. Role of surgical outcome as prognostic factor in advanced epithelial ovarian cancer: a combined exploratory analysis of 3 prospectively randomized phase 3 multicenter trials: by the Arbeitsgemeinschaft Gynaekologische Onkologie Studiengruppe Ovarialkarzinom (AGO-OVAR) and the Groupe d'Investigateurs Nationaux Pour les Etudes des Cancers de l'Ovaire (GINECO). Cancer. 2009;115(6):1234–44. [PubMed: 19189349]
3. Li SS, Ma J, Wong AST. Chemoresistance in ovarian cancer: exploiting cancer stem cell metabolism. J Gynecol Oncol. 2018;29(2):e32. [PubMed: 29468856]
4. Bapat SA, Mali AM, Koppikar CB, Kurrey NK. Stem and progenitor-like cells contribute to the aggressive behavior of human epithelial ovarian cancer. Cancer research. 2005;65(8):3025–9. [PubMed: 15833827]
5. Zhang S, Balch C, Chan MW, Lai HC, Matei D, Schilder JM, et al. Identification and characterization of ovarian cancer-initiating cells from primary human tumors. Cancer research. 2008;68(11):4311–20. [PubMed: 18519691]
6. Silva IA, Bai S, McLean K, Yang K, Griffith K, Thomas D, et al. Aldehyde dehydrogenase in combination with CD133 defines angiogenic ovarian cancer stem cells that portend poor patient survival. Cancer research. 2011;71(11):3991–4001. [PubMed: 21498635]
7. Gao MQ, Choi YP, Kang S, Youn JH, Cho NH. CD24+ cells from hierarchically organized ovarian cancer are enriched in cancer stem cells. Oncogene. 2010;29(18):2672–80. [PubMed: 20190812]
8. Condello S, Morgan CA, Nagdas S, Cao L, Turek J, Hurley TD, et al. beta-Catenin-regulated ALDH1A1 is a target in ovarian cancer spheroids. Oncogene. 2015;34(18):2297–308. [PubMed: 24954508]
9. Vassalli G Aldehyde Dehydrogenases: Not Just Markers, but Functional Regulators of Stem Cells. Stem Cells Int. 2019;2019:3904645. [PubMed: 30733805]
10. Kim D, Choi BH, Ryoo IG, Kwak MK. High NRF2 level mediates cancer stem cell-like properties of aldehyde dehydrogenase (ALDH)-high ovarian cancer cells: inhibitory role of all-trans retinoic acid in ALDH/NRF2 signaling. Cell Death Dis. 2018;9(9):896. [PubMed: 30166520]
11. Wang Y, Zhao G, Condello S, Huang H, Cardenas H, Tanner EJ, et al. Frizzled-7 Identifies Platinum-Tolerant Ovarian Cancer Cells Susceptible to Ferroptosis. Cancer research. 2021;81(2):384–99. [PubMed: 33172933]
12. Xia Y, Wei X, Gong H, Ni Y. Aldehyde dehydrogenase serves as a biomarker for worse survival profiles in ovarian cancer patients: an updated meta-analysis. BMC Womens Health. 2018;18(1):199. [PubMed: 30522488]

13. Wainwright EN, Scaffidi P. Epigenetics and Cancer Stem Cells: Unleashing, Hijacking, and Restricting Cellular Plasticity. Trends Cancer. 2017;3(5):372–86. [PubMed: 28718414]
14. Toh TB, Lim JJ, Chow EK. Epigenetics in cancer stem cells. Mol Cancer. 2017;16(1):29. [PubMed: 28148257]
15. Cao Q, Yu J, Dhanasekaran SM, Kim JH, Mani RS, Tomlins SA, et al. Repression of E-cadherin by the polycomb group protein EZH2 in cancer. Oncogene. 2008;27(58):7274–84. [PubMed: 18806826]
16. Wang Y, Cardenas H, Fang F, Condello S, Taverna P, Segar M, et al. Epigenetic targeting of ovarian cancer stem cells. Cancer research. 2014;74(17):4922–36. [PubMed: 25035395]
17. Zong X, Wang W, Ozes A, Fang F, Sandusky GE, Nephew KP. EZH2-Mediated Downregulation of the Tumor Suppressor DAB2IP Maintains Ovarian Cancer Stem Cells. Cancer research. 2020;80(20):4371–85. [PubMed: 32816909]
18. Feng Q, Wang HB, Ng HH, Erdjument-Bromage H, Tempst P, Struhl K, et al. Methylation of H3-lysine 79 is mediated by a new family of HMTases without a SET domain. Current Biology. 2002;12(12):1052–8. [PubMed: 12123582]
19. Nguyen AT, Zhang Y. The diverse functions of Dot1 and H3K79 methylation. Genes & development. 2011;25(13):1345–58. [PubMed: 21724828]
20. Okada Y, Feng Q, Lin Y, Jiang Q, Li Y, Coffield VM, et al. hDOT1L links histone methylation to leukemogenesis. Cell. 2005;121(2):167–78. [PubMed: 15851025]
21. Stein EM, Garcia-Manero G, Rizzieri DA, Tibes R, Berdeja JG, Savona MR, et al. The DOT1L inhibitor pinometostat reduces H3K79 methylation and has modest clinical activity in adult acute leukemia. Blood. 2018;131(24):2661–9. [PubMed: 29724899]
22. Alexandrova E, Salvati A, Pecoraro G, Lamberti J, Melone V, Sellitto A, et al. Histone Methyltransferase DOT1L as a Promising Epigenetic Target for Treatment of Solid Tumors. Front Genet. 2022;13:864612. [PubMed: 35495127]
23. Nassa G, Salvati A, Tarallo R, Gigantino V, Alexandrova E, Memoli D, et al. Inhibition of histone methyltransferase DOT1L silences ERalpha gene and blocks proliferation of antiestrogen-resistant breast cancer cells. Sci Adv. 2019;5(2):eaav5590. [PubMed: 30775443]
24. Cho MH, Park JH, Choi HJ, Park MK, Won HY, Park YJ, et al. DOT1L cooperates with the c-Myc-p300 complex to epigenetically derepress CDH1 transcription factors in breast cancer progression. Nat Commun. 2015;6:7821. [PubMed: 26199140]
25. Zhang X, Liu D, Li M, Cao C, Wan D, Xi B, et al. Prognostic and therapeutic value of disruptor of telomeric silencing-1-like (DOT1L) expression in patients with ovarian cancer. J Hematol Oncol. 2017;10(1):29. [PubMed: 28114995]
26. Chava S, Bugide S, Edwards YJK, Gupta R. Disruptor of telomeric silencing 1-like promotes ovarian cancer tumor growth by stimulating pro-tumorigenic metabolic pathways and blocking apoptosis. Oncogenesis. 2021;10(7):48. [PubMed: 34253709]
27. Dong R, Qiang W, Guo H, Xu X, Kim JJ, Mazar A, et al. Histologic and molecular analysis of patient derived xenografts of high-grade serous ovarian carcinoma. J Hematol Oncol. 2016;9(1):92. [PubMed: 27655386]
28. Li J, Condello S, Thomes-Pepin J, Ma X, Xia Y, Hurley TD, et al. Lipid Desaturation Is a Metabolic Marker and Therapeutic Target of Ovarian Cancer Stem Cells. Cell Stem Cell. 2017;20(3):303–14 e5. [PubMed: 28041894]
29. Hu Y, Smyth GK. ELDA: extreme limiting dilution analysis for comparing depleted and enriched populations in stem cell and other assays. J Immunol Methods. 2009;347(1–2):70–8. [PubMed: 19567251]
30. Integrated genomic analyses of ovarian carcinoma. Nature. 2011;474(7353):609–15. [PubMed: 21720365]
31. Gyorffy B, Lanczky A, Szallasi Z. Implementing an online tool for genome-wide validation of survival-associated biomarkers in ovarian-cancer using microarray data from 1287 patients. Endocr Relat Cancer. 2012;19(2):197–208. [PubMed: 22277193]
32. Ghandi M, Huang FW, Jane-Valbuena J, Kryukov GV, Lo CC, McDonald ER 3rd, et al. Next-generation characterization of the Cancer Cell Line Encyclopedia. Nature. 2019;569(7757):503–8. [PubMed: 31068700]

33. Landen CN Jr., Goodman B, Katre AA, Steg AD, Nick AM, Stone RL, et al. Targeting aldehyde dehydrogenase cancer stem cells in ovarian cancer. Mol Cancer Ther. 2010;9(12):3186–99. [PubMed: 20889728]
34. Lim E, Wu D, Pal B, Bouras T, Asselin-Labat ML, Vaillant F, et al. Transcriptome analyses of mouse and human mammary cell subpopulations reveal multiple conserved genes and pathways. Breast Cancer Res. 2010;12(2):R21. [PubMed: 20346151]
35. Boquest AC, Shahdadfar A, Fronsdal K, Sigurjonsson O, Tunheim SH, Collas P, et al. Isolation and transcription profiling of purified uncultured human stromal stem cells: alteration of gene expression after in vitro cell culture. Mol Biol Cell. 2005;16(3):1131–41. [PubMed: 15635089]
36. Meyers RM, Bryan JG, McFarland JM, Weir BA, Sizemore AE, Xu H, et al. Computational correction of copy number effect improves specificity of CRISPR-Cas9 essentiality screens in cancer cells. Nature genetics. 2017;49(12):1779–84. [PubMed: 29083409]
37. Liu D, Zhang XX, Li MC, Cao CH, Wan DY, Xi BX, et al. C/EBPbeta enhances platinum resistance of ovarian cancer cells by reprogramming H3K79 methylation. Nat Commun. 2018;9(1):1739. [PubMed: 29712898]
38. Kryczek I, Lin Y, Nagarsheth N, Peng D, Zhao L, Zhao E, et al. IL-22(+)CD4(+) T cells promote colorectal cancer stemness via STAT3 transcription factor activation and induction of the methyltransferase DOT1L. Immunity. 2014;40(5):772–84. [PubMed: 24816405]
39. MacLeod G, Bozek DA, Rajakulendran N, Monteiro V, Ahmadi M, Steinhart Z, et al. Genome-Wide CRISPR-Cas9 Screens Expose Genetic Vulnerabilities and Mechanisms of Temozolomide Sensitivity in Glioblastoma Stem Cells. Cell Rep. 2019;27(3):971–86 e9. [PubMed: 30995489]
40. Kurani H, Razavipour SF, Harikumar KB, Dunworth M, Ewald AJ, Nasir A, et al. DOT1L Is a Novel Cancer Stem Cell Target for Triple-Negative Breast Cancer. Clinical cancer research : an official journal of the American Association for Cancer Research. 2022;28(9):1948–65. [PubMed: 35135840]
41. Wang X, Wang H, Xu B, Jiang D, Huang S, Yu H, et al. Depletion of H3K79 methyltransferase Dot1L promotes cell invasion and cancer stem-like cell property in ovarian cancer. Am J Transl Res. 2019;11(2):1145–53. [PubMed: 30899413]
42. Nagaraj AB, Joseph P, Kovalenko O, Singh S, Armstrong A, Redline R, et al. Critical role of Wnt/beta-catenin signaling in driving epithelial ovarian cancer platinum resistance. Oncotarget. 2015;6(27):23720–34. [PubMed: 26125441]
43. Nguyen VHL, Hough R, Bernaudo S, Peng C. Wnt/beta-catenin signalling in ovarian cancer: Insights into its hyperactivation and function in tumorigenesis. J Ovarian Res. 2019;12(1):122. [PubMed: 31829231]
44. Yoshioka S, King ML, Ran S, Okuda H, MacLean JA 2nd, McAsey ME, et al. WNT7A regulates tumor growth and progression in ovarian cancer through the WNT/beta-catenin pathway. Mol Cancer Res. 2012;10(3):469–82. [PubMed: 22232518]
45. Condello S, Cao L, Matei D. Tissue transglutaminase regulates beta-catenin signaling through a c-Src-dependent mechanism. FASEB J. 2013;27(8):3100–12. [PubMed: 23640056]
46. Zhu J, Zhang S, Gu L, Di W. Epigenetic silencing of DKK2 and Wnt signal pathway components in human ovarian carcinoma. Carcinogenesis. 2012;33(12):2334–43. [PubMed: 22964660]
47. Fine-tuning epigenome editors. Nature biotechnology. 2022;40(3):281.
48. Glasspool RM, Brown R, Gore ME, Rustin GJ, McNeish IA, Wilson RH, et al. A randomised, phase II trial of the DNA-hypomethylating agent 5-aza-2'-deoxycytidine (decitabine) in combination with carboplatin vs carboplatin alone in patients with recurrent, partially platinum-sensitive ovarian cancer. Br J Cancer. 2014;110(8):1923–9. [PubMed: 24642620]
49. Oza AM, Matulonis UA, Alvarez Secord A, Nemunaitis J, Roman LD, Blagden SP, et al. A Randomized Phase II Trial of Epigenetic Priming with Guadecitabine and Carboplatin in Platinum-resistant, Recurrent Ovarian Cancer. Clinical cancer research : an official journal of the American Association for Cancer Research. 2020;26(5):1009–16. [PubMed: 31831561]
50. Dizon DS, Damstrup L, Finkler NJ, Lassen U, Celano P, Glasspool R, et al. Phase II activity of belinostat (PXD-101), carboplatin, and paclitaxel in women with previously treated ovarian cancer. Int J Gynecol Cancer. 2012;22(6):979–86. [PubMed: 22694911]

Implication:

This study found that the histone methyltransferase DOT1L regulates the self-renewal and tumor initiation capacity of ovarian CSCs and suggests DOT1L as a new cancer target.

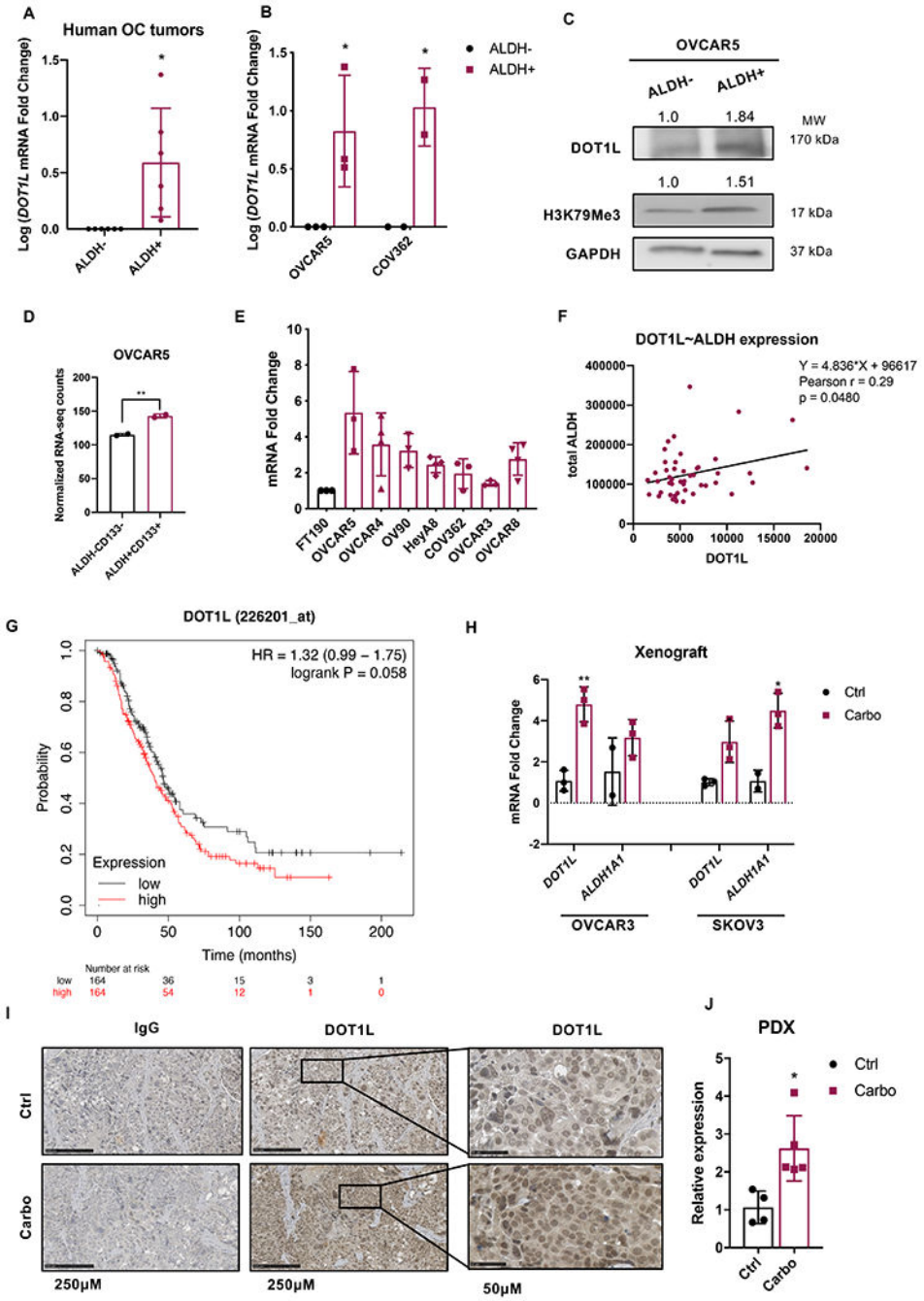

Figure 1. DOT1L is enriched in ALDH+ ovarian CSCs and in carboplatin treated tumors.

A, B, qRT-PCR quantification of *DOT1L* expression in ALDH+ ovarian CSCs and ALDH− non-stem cells sorted from primary HGSOC tumors (n = 6) (**A**), or OVCAR5 (n=3) and COV362 (n=2) OC cell lines (**B**). **C**, Western blot measured DOT1L and H3K79Me3 protein levels in ALDH+ ovarian CSCs and ALDH− cells sorted from OVCAR5 cells. Densitometry using ImageJ quantifies DOT1L expression and H3K79Me3 levels relative to GAPDH. **D**, Normalized RNA-seq counts of ALDH+CD133+ and ALDH−CD133− cells sorted from OVCAR5 (n = 2). **E**, qRT-PCR analysis of *DOT1L* expression in human fallopian tube

epithelial (FT190) and OC cell lines: OVCAR5, OVCAR4, OV90, HeyA8m COV362, OVCAR3, OVCAR8. **F**, Correlation between *DOT1L* expression and expression levels of genes from the ALDH family among 47 OC cell lines from CCLE. **G**, Overall survival (OS) according to DOT1L expression using the Kaplan-Meier method with log-rank test (top 25 percentile vs. bottom 25 percentile, n = 655) in OC samples from GEO databases described in Materials and Methods. **H**, Expression levels of *DOT1L* and *ALDH1A1* mRNA measured by qRT-PCR in OVCAR3 and SKOV3 xenografts treated with carboplatin (Carbo) or PBS control (Ctrl) (n = 3 for *DOT1L*, n = 2 for *ALDH1A1*). **I**, Representative images of IHC for DOT1L in PDX tumors treated with carboplatin (Carbo) or PBS (Ctrl). **J**, mRNA expression levels of *DOT1L* in PDX tumors from mice treated with carboplatin (Carbo) or PBS control (Ctrl) measured by qRT-PCR (n = 3 for Ctrl, n = 2 for Carbo). Data are shown as means ± SD of all biological replicates. * and ** represent $P < 0.05$ and $P < 0.01$ respectively.

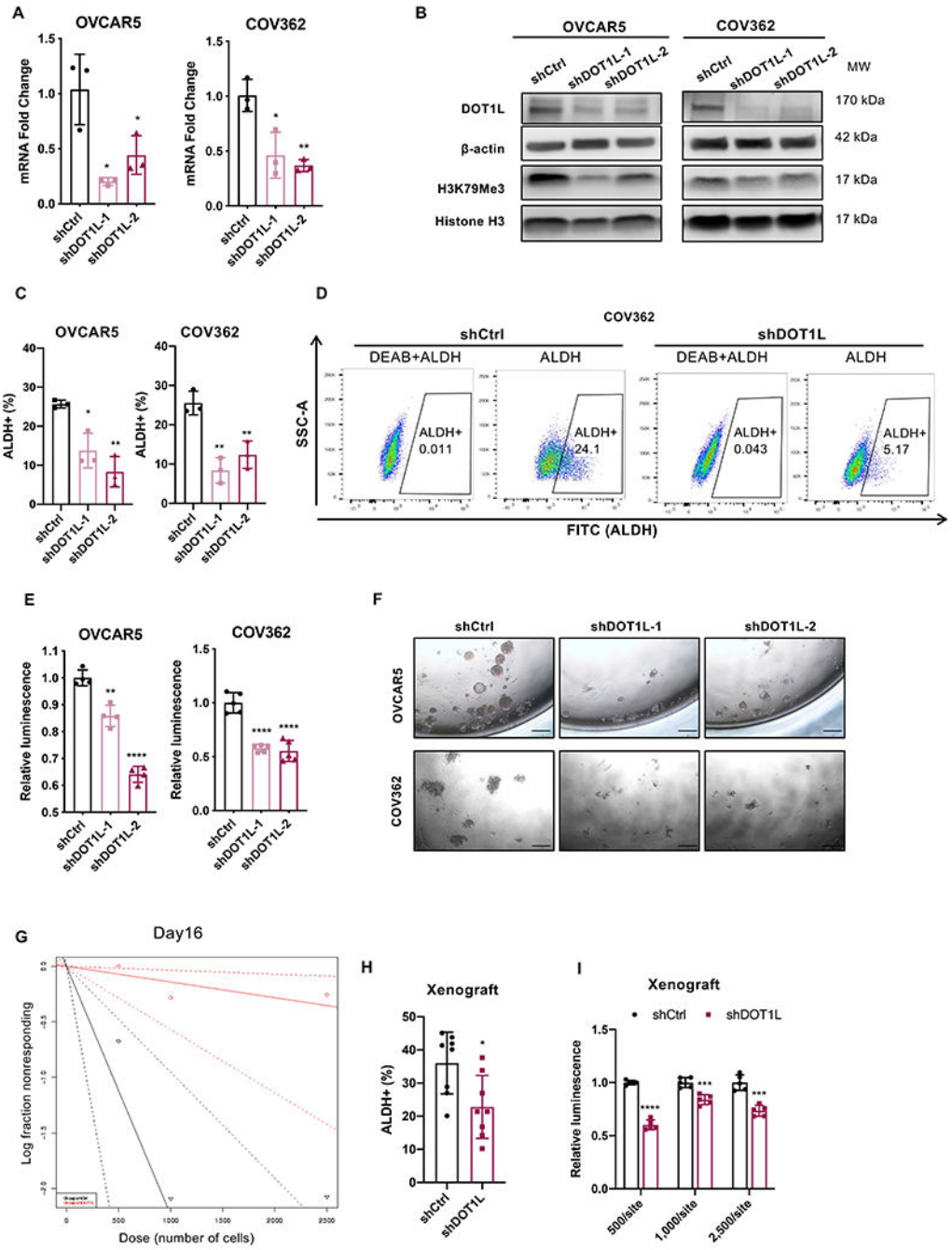

Figure 2. DOT1L knockdown reduces stemness in OC

A, Measurement by qRT-PCR of *DOT1L* gene expression in OVCAR5 and COV362 cells transduced with shRNAs targeting DOT1L (shDOT1L-1 or shDOT1L-2) or with control shRNAs (shCtrl) (n = 3). **B**, Western blotting of DOT1L and H3K79Me3 protein levels in shDOT1L and shCtrl stably transduced OC cell lines. **C**, Percentages of ALDH+ ovarian CSCs measured by flow cytometry in shDOT1L and shCtrl stably transduced OVCAR5 and COV362 cells (n = 3). **D**, Representative flow cytometry analysis of ALDH+ CSCs in shDOT1L and shCtrl COV362 cells. **E**, Assessment of spheroid formation in vitro by

measuring cell viability (CellTiter Glo 3D assay) in shDOT1L and shCtrl OVCAR5 (n = 4) and COV362 cells (n = 5). **F**, Representative images of spheroids formed by shDOT1L and shCtrl stably transduced OC cells. **G**, Log-fraction plot shows tumor initiation in mice injected with shCtrl and shDOT1L transduced OVCAR5 cells (n = 12). **H**, ALDH+ CSCs population from xenograft tumors collected from (**G**) (n=8). **I**, Estimation of spheroid formation based on cell viability quantified through the CellTiter Glo 3D viability assay. Cells were isolated from xenograft tumors from **G**, counted and cultured in non-adherent plates and Mammocult media (n=5). Equal numbers of cells (5000 cells/well) were plated for each category of xenograft tumors. Data are shown as means ± SD of biological replicates. *, **, *** and **** represent P <0.05, P< 0.01, P< 0.005 and P< 0.001, respectively.

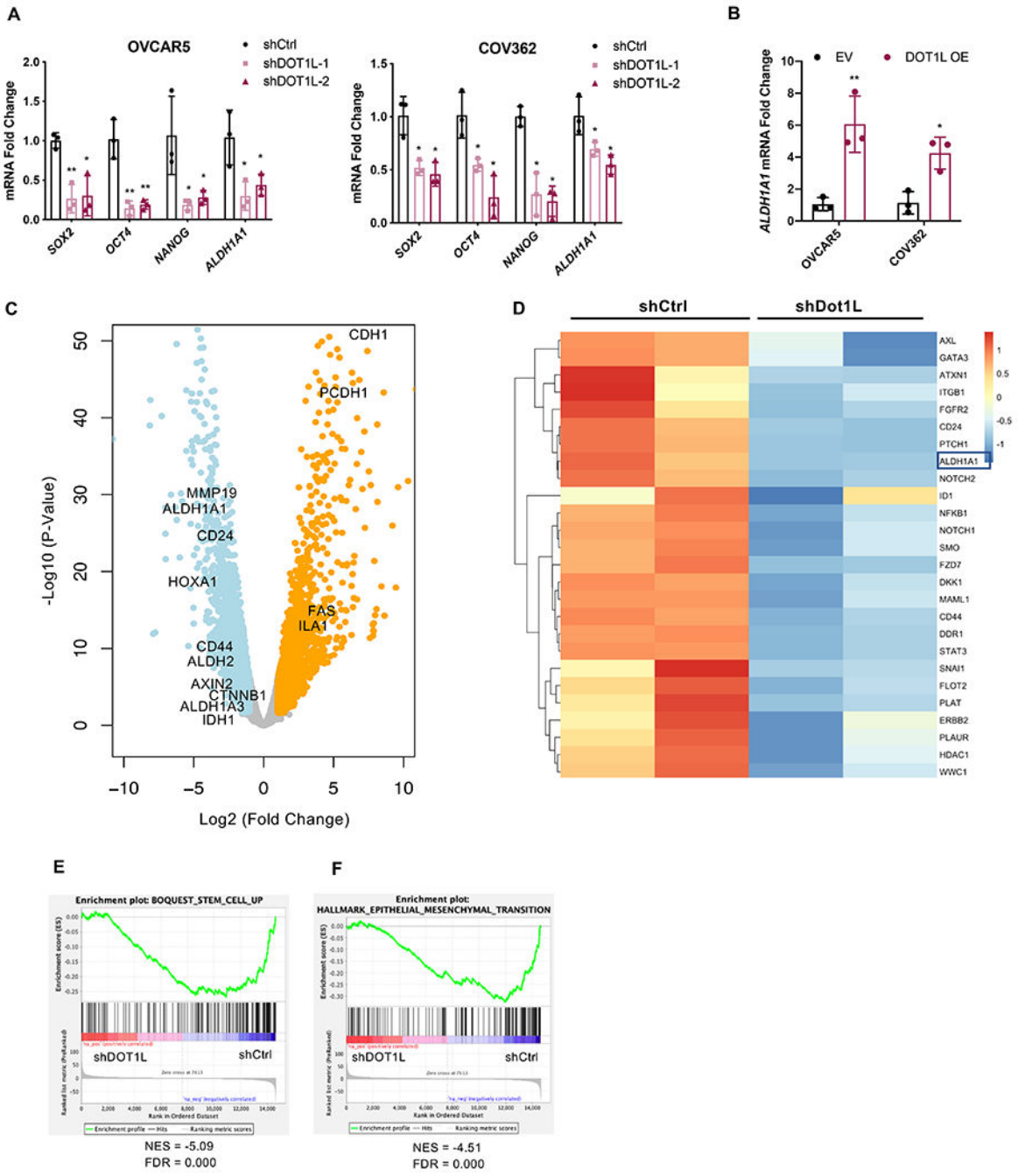

Figure 3. DOT1L regulates expression of stemness-associated genes in ovarian CSCs

A, mRNA expression levels of stemness-associated genes (*SOX2, OCT4, NANOG*), and *ALDH1A1* stem cell marker in OVCAR5 and COV362 cells transduced with shRNAs directed at DOT1L (shDOT1L) or control shRNAs (shCtrl) (n = 3). **B**, Expression of *ALDH1A1* mRNA in OVCAR5 and COV362 cells transduced with a DOT1L expression vector (DOT1L-OE) or empty vector (EV) (n = 3) measured by qRT-PCR. **C**, Volcano plot shows differentially expressed genes in shDOT1L vs shCtrl transduced OVCAR5 cells. **D**, Heatmap of the top 25 downregulated genes among stemness-associated genes

in shDOT1L vs. shCtrl transduced OVCAR5 cells. Gene expression was measured by RNA-seq. **E-F**, GSEA enrichment plot for "*Boquest stem cell up*" (**E**) and "*hallmark epithelial-mesenchymal transition*" (**F**) gene sets in shDOT1L versus shCtrl transduced OVCAR5 cells. Data are shown as means ± SD of biological replicates. * and ** indicate $P < 0.05$ and $P < 0.01$, respectively.

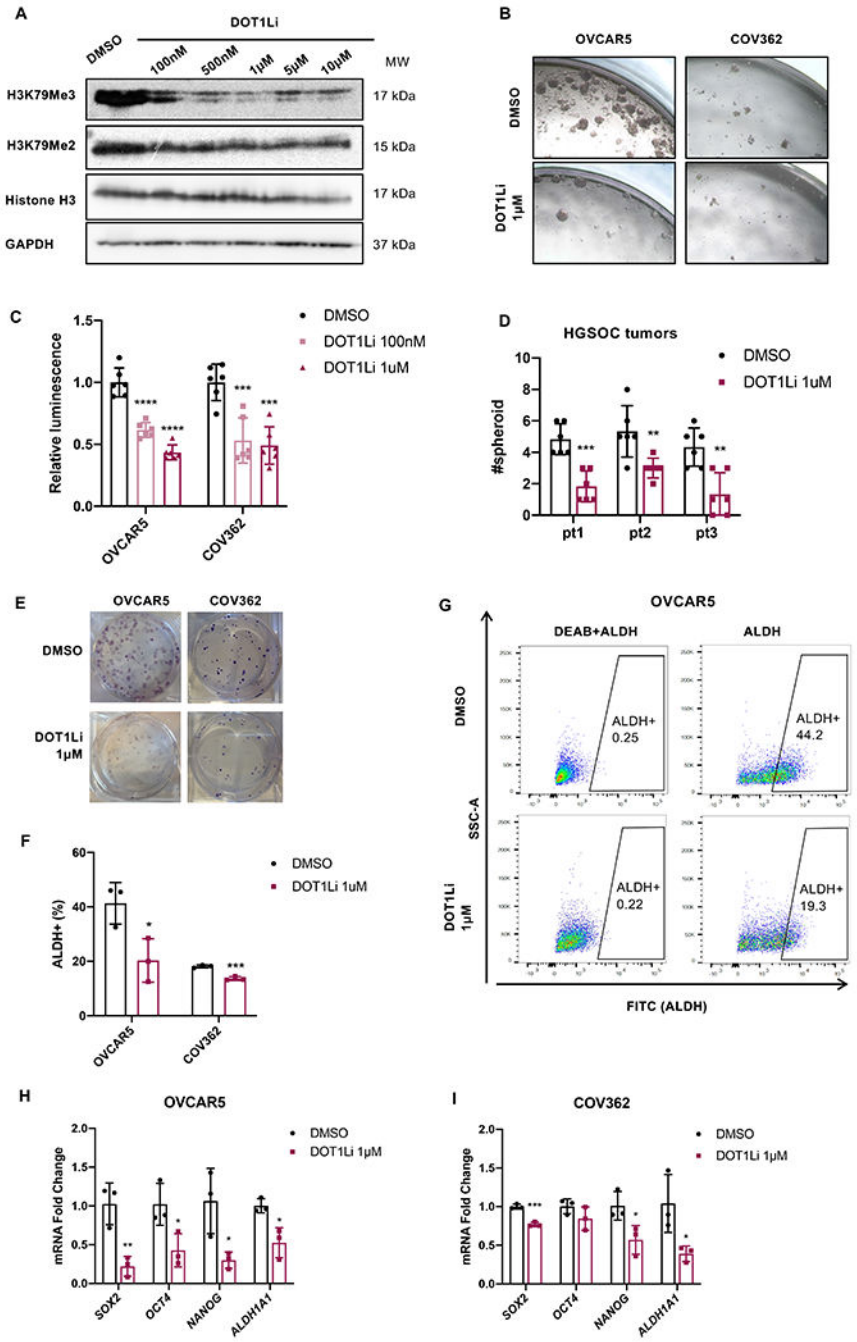

Figure 4. Inhibition of DOT1L reduces the CSCs population and expression of stemness-associated genes

A, Western blot analysis of H3K79Me3 and H3K79Me2 protein levels in OVCAR5 cells treated with different doses of DOT1L inhibitor EPZ-5676 (DOT1Li) or DMSO for 5 days. **B**, **C**, Representative images (**B**) and estimation of spheroid formation based on cell viability (CellTiter Glo 3D assay) in OVCAR5 and COV362 cells treated with DOT1Li (1μM) or DMSO. **D**, Numbers of spheroids formed by cells isolated from primary HGSOC tumors and treated with DOT1Li as in C (n = 3). **E**, Representative pictures of a clonogenic

survival assay with OVCAR5, COV362 and OVCAR3 cells treated with 1μM DOT1Li. **F, G**, Percentages (**F**) and representative analysis (**G**) of ALDH+ ovarian CSCs determined by FACS in OVCAR5 and COV362 cells treated with 1μM DOT1Li (n = 3). **H, I**, *mRNA* expression levels of *SOX2*, *OCT4*, *NANOG* and *ALDH1A1* in OVCAR5 (**H**) and COV362 (**I**) cells treated with DMSO or DOT1Li (1μM) for 5 days. Data are shown as means ± SD of biological replicates. *, **, *** and **** depict $P<0.05$, $P< 0.01$, $P< 0.005$ and $P< 0.001$ respectively.

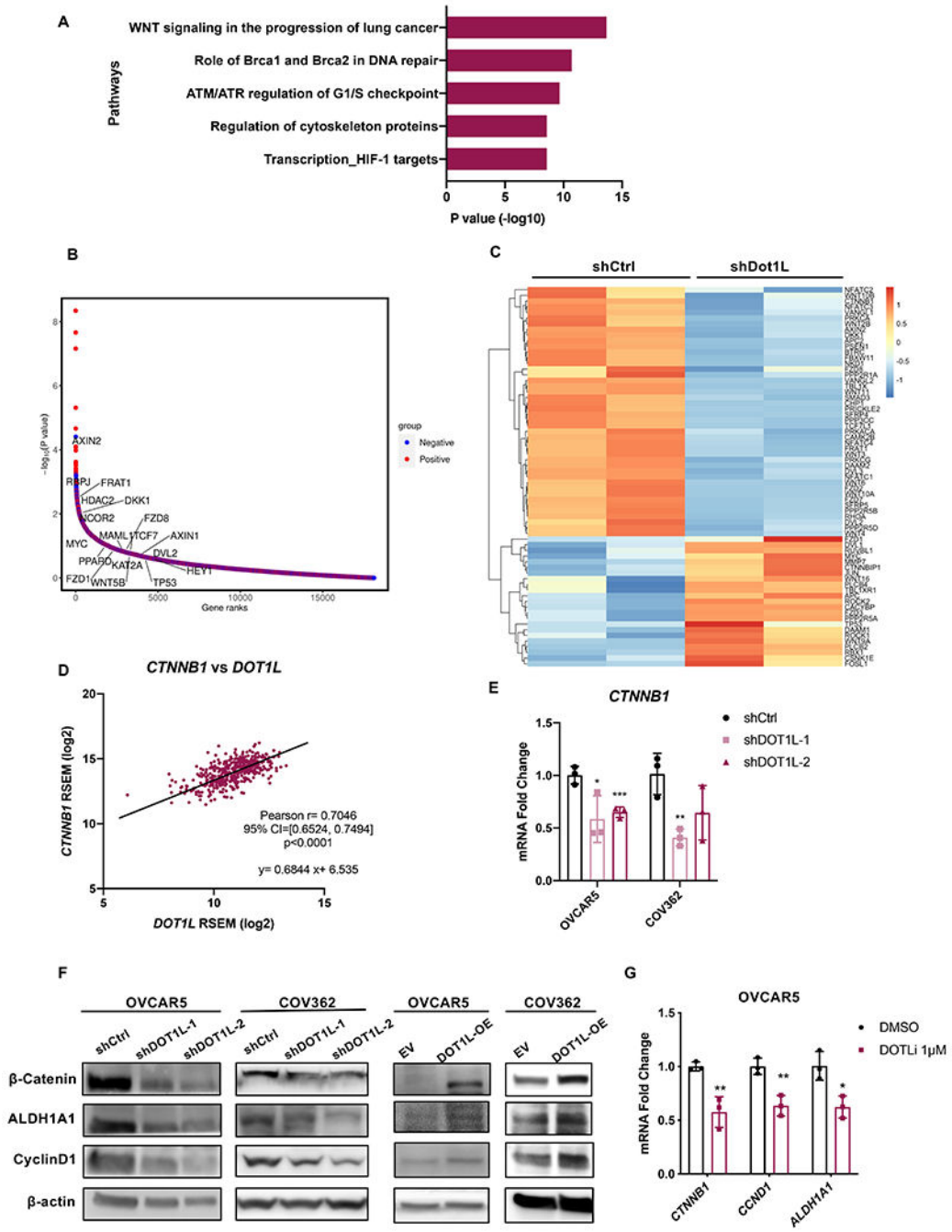

Figure 5. DOT1L regulates stemness of CSCs by upregulating β-catenin

A, Top 5 enriched pathways identified by MetaCore analysis of differentially expressed genes measured by RNA-seq in shDOT1L vs. shCtrl transduced OVCAR5 cells (n = 2). **B**, Dependency and ranks of KEGG Wnt canonical signaling pathway (hsa04310) genes as they related to DOT1L in OC cell lines profiled in CCLE. **C**, Heat map shows expression of genes in the KEGG Wnt canonical signaling pathway based on RNA-seq analysis of shDOT1L and shCtrl OVCAR5 cells. **D**, A scatter plot shows the correlation between expression levels of *CTNNB1* and *DOT1L* in OC samples from TCGA (n = 427). **E**,

mRNA expression levels of *CTNNB1* in shDOT1L and shCtrl cells (n = 3) OC cell lines (OVCAR5, COV362) measured by qRT-PCR. **F**, Western blot analysis of Wnt pathway proteins (β-Catenin, Cyclin D1) and stem cell marker ALDH1A1 in shDOT1L vs shCtrl transduced OC cells (left) and in cells overexpressing DOT1L (DOT1L-OE) vs control (EV) (right). **G**, *mRNA* expression levels of *CTNNB1*, *CCND1*, and *ALDH1A1* in OVCAR5 cells treated with 1μM DOT1Li (n = 3). Data are shown as means ± SD of biological replicates. *, ** and *** depict $P < 0.05$, $P < 0.01$ and $P < 0.005$ respectively.

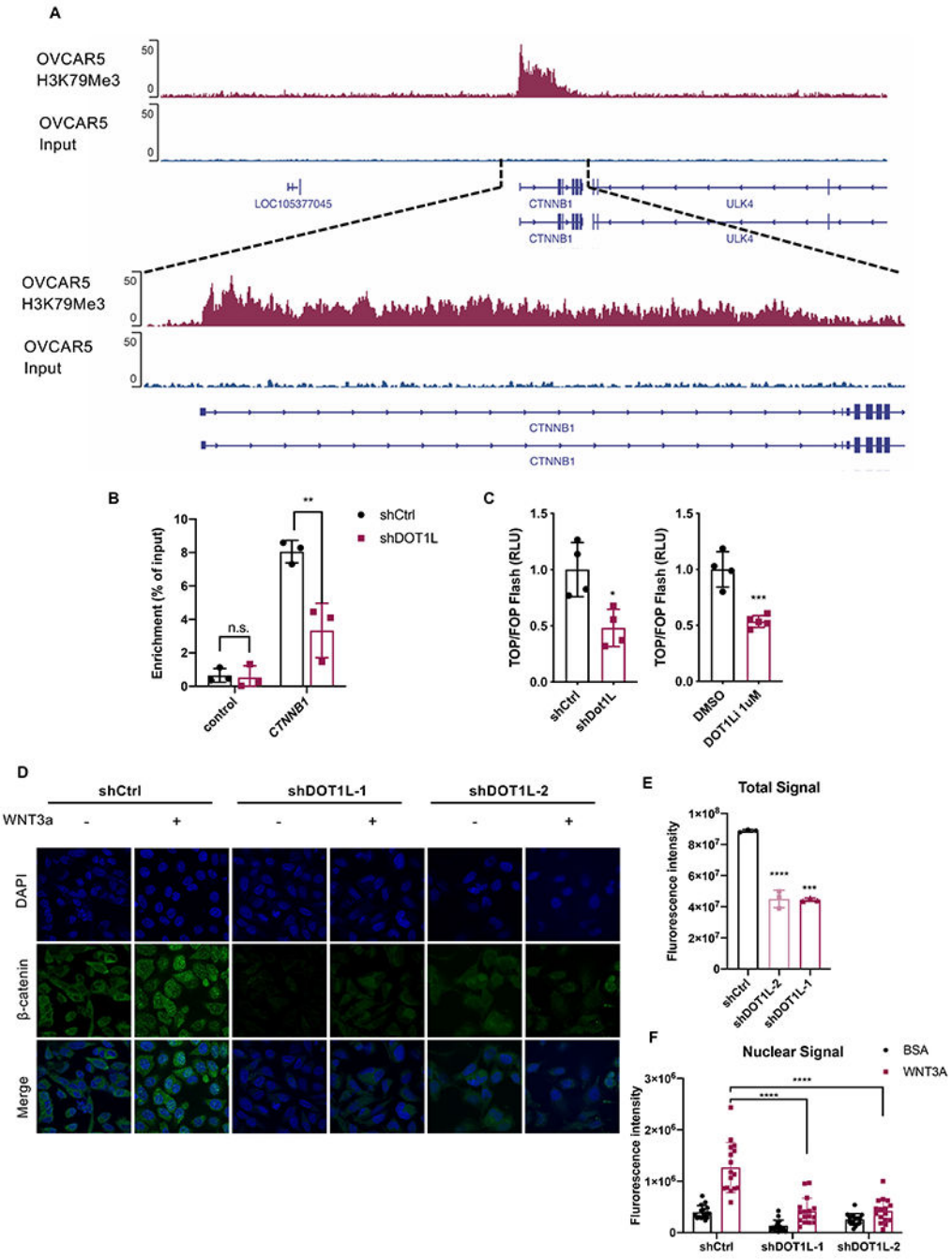

Figure 6. DOT1L regulates β-catenin through enrichment of H3K79Me3 at the CTNNB1 promoter

A, Track view of H3K79Me3 enrichment at the promoter of the *CTNNB1* gene as determined by ChIP-seq in OVCAR5 cells. **B**, ChIP-qPCR analysis shows enrichment of H3K79Me3 at the promoter of the *CTNNB1* in OVCAR5 cells transduced with shRNAs directed at DOT1L (shDOT1L) or control shRNAs (shCtrl) (n = 3). **C**, Relative luminescence intensity of shDOT1L vs. shCtrl OVCAR5 cells transfected with TOPFlash luciferase reporter or FOPFlash mutant reporter, and OVCAR5 cells transfected with

TOPFlash luciferase reporter or FOPFlash mutant reporter and then treated with DOT1Li or DMSO (n = 4). **D**, Immunofluorescence staining of β-catenin (Alexa Flour 488, green) and DAPI (blue) in shDOT1L and shCtrl OVCAR5 cells treated with 100μg/ml WNT3a (+) or BSA control (–). Nuclear β-catenin localization is identified by the cyan color on merged images (100X). **E**, Quantification of the cellular IF signal for β-catenin by using Image J in shCtrl and shDOT1L cells under basal conditions (n = 3). **F**, Quantification of the nuclear IF signal for β-catenin in shDOT1L and shCtrl OVCAR5 cells treated with 100μg/ml WNT3a (+) or BSA by using Image J. Data are shown as means ± SD, *** corresponds to $P < 0.005$.

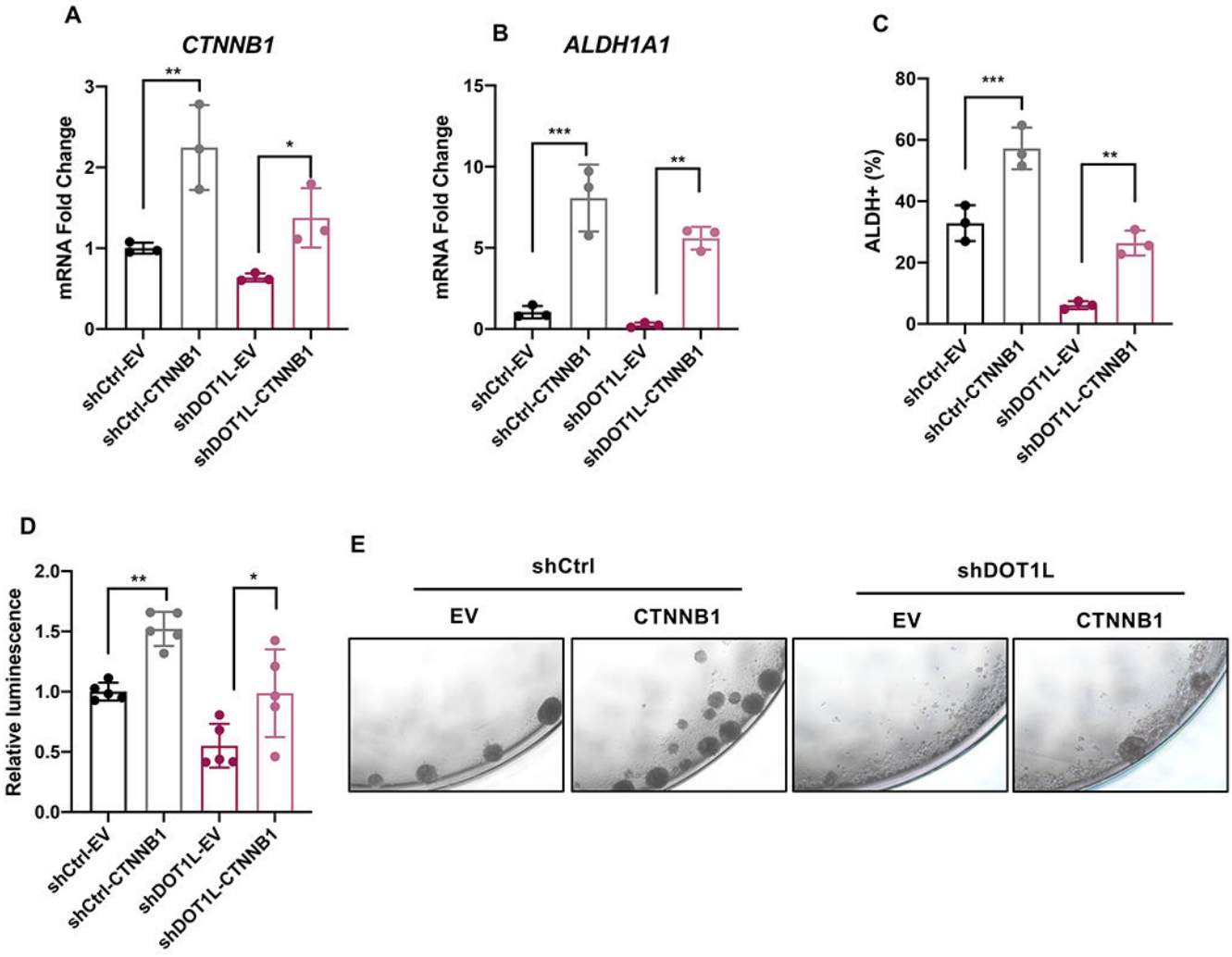

Figure 7. Effects of β-Catenin downstream of DOT1L

A, B, *mRNA* expression levels of *CTNNB1* (**A**) and *ALDH1A1* (**B**) determined by qRT-PCR (n = 3) in shDOT1L-transduced OVCAR5 cells transfected with *CTNNB1*-expressing vector (shDOT1L-CTNNB1) or empty vector (shDOT1L-EV) and in shCtrl cells transfected with empty vector (shCtrl-EV). **C**, ALDH+ population measured by flow cytometry in shCtrl-EV, shDOT1L-EV, or shDOT1L-CTNNB1 cells. **D**, spheroid formation measured by CellTiter Glo 3D and **E**, pictures of spheroids (20X magnification), in shCtrl-EV, shDOT1L-EV, or shDOT1L-CTNNB1 cells. For all panels: data are shown as means ± SD, * $p<0.05$, ** $p<0.01$, *** $p<0.005$.